Wavelet-based Contourlet Coding Using an SPIHT-like Algorithm

Ramin Eslami and Hayder Radha

ECE Department, Michigan State University, East Lansing, MI 48824, USA
Emails: {eslamira, radha}@egr.msu.edu

***Abstract*—In this paper, we propose a new non-linear image approximation method that decomposes images both radially and angularly. Our approximation is based on two stages of filter banks that are non-redundant and perfect reconstruction and therefore lead to an overall non-redundant and perfect reconstruction transform. We show that this transform, which we call it the *Wavelet-Based Contourlet Transform* (WBCT), is capable of efficiently approximating natural images containing contours and oscillatory patterns. In addition, we propose a new image coding scheme based on the proposed transform using a new set partitioning in hierarchical trees (SPIHT) algorithm that provides an embedded code. Due to differences in parent-child relationships between the WBCT coefficients and wavelet coefficients, we develop an elaborated repositioning algorithm for the WBCT coefficients in such a way that we could consider spatial orientation trees that are similar to the original SPIHT algorithm. Our experiments demonstrate that the proposed approach is efficient in coding images that possess mostly textures and contours. Our simulation results also show that this new coding approach is competitive to the wavelet coder in terms of the PSNR-rate curves, and is visually superior to the wavelet coder for the mentioned images.**

I. Introduction

Although the wavelet transform is proved to be powerful in many signal and image processing applications such as compression, noise removal, image edge enhancement, and feature extraction; wavelets are not optimal in capturing the two-dimensional singularities found in images. In particular, natural images consist of edges that are smooth curves and which cannot be captured efficiently by the wavelet transform. Therefore, several new transforms have been proposed for image signals.

The contourlet transform is one of the new geometrical image transforms, which can efficiently represent images containing contours and textures [3][5][6]. This transform uses a structure similar to that of curvelets [1], that is, a stage of subband decomposition followed by a directional transform. In the contourlet transform, a Laplacian pyramid is employed for the first stage, while directional filter banks (DFB) are used in the angular decomposition stage. Due to the redundancy of the Laplacian pyramid, the contourlet transform has a redundancy factor of 4/3 and hence, it may not be the optimum choice for image coding applications.

Recently, some approaches have been attempted to introduce non-redundant image transforms based on DFB with the capability of both radial and angular decomposition. The octave-band directional filter banks [7] are a new family of directional filter banks that offer an octave-band radial decomposition as well. Using a three-band (three non-uniform bands) DFB, one can decompose the output of a DFB to a lowpass band and two highpass bands. The lowpass band can be decomposed further using another three-band DFB with a bandwidth that is half of the former three-band DFB; thus providing a radial decomposition on the directional components. Another approach is the critically sampled contourlet (CRISP-contourlet) transform [9], which is realized using a one-stage non-separable filter bank. Using similar frequency decomposition to that of the contourlet transform, it provides a non-redundant version of the contourlet transform.

In this paper we propose a new non-redundant image transform, the *Wavelet-Based Contourlet Transform* (WBCT), with a construction similar to the contourlet transform. The proposed WBCT achieves both radial and angular decomposition to an arbitrary extent and obeys the anisotropy scaling law of $width \approx length^2$ [1]. Compared to the aforementioned DFB-based non-redundant transforms, the WBCT can easily be realized by applying DFB on the wavelet coefficients of an image.

In a previous attempt [5], the contourlet transform is employed in a direct transform-based image coding scheme and is shown that despite its redundancy, it is capable of preserving more textures and details when compared to a direct transform wavelet coder. In this work, to improve the performance of the mentioned contourlet coder, we used the non-redundant WBCT in conjunction with an SPIHT algorithm [14] to construct an embedded image coder. Due to differences in parent-child relationships between the WBCT coefficients and wavelet coefficients, we developed an elaborated repositioning algorithm for the WBCT coefficients in such a way that we could have similar *spatial orientation trees* [14] (the *zero-trees* introduced in [15]) as the ones used for scanning the wavelet coefficients. Our simulation results show that the proposed coder is competitive to the original SPIHT coder, especially for a category of images that have a significant amount of textures and oscillatory patterns and therefore are not “wavelet-friendly” images.

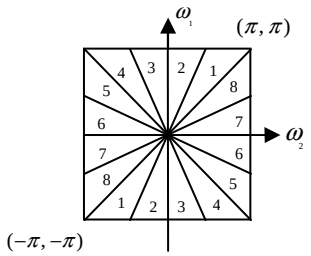

Fig. 1. Directional filter bank frequency partitioning.

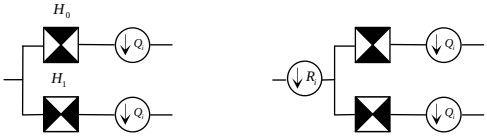

Fig. 2. Building blocks of the DFB (synthesis part). *Left:* quincunx filter bank required for the first two levels. *Right:* resampling followed by the quincunx filter bank required for levels three and higher.

The remainder of the paper is organized as follows. The next section briefly explains the WBCT and its construction. Section 3 describes the proposed WBCT-based coding approach including a new SPIHT-like repositioning/scanning algorithm of the non-redundant WBCT coefficients. Section 4 illustrates some of the simulation and numerical results achieved by this coder and finally the main conclusions are outlined in Section 5.

II. The Wavelet-Based Contourlet Transform

Similar to the contourlet transform, the WBCT consists of two filter bank stages. The first stage provides subband decomposition, which in the case of the WBCT is a wavelet transform, in contrast to the Laplacian pyramid used in contourlets. The second stage of the WBCT is a directional filter bank (DFB), which provides angular decomposition (Fig. 1). The first stage is realized by separable filter banks, while we implement the second stage using non-separable filter banks.

For the DFB stage, we employ the iterated tree-structured filter banks using fan filters [11][3][4]. For the first two levels, it is sufficient to use a simple quincunx filter bank. For higher levels of the wavelet decomposition, we use another building block, which is resampling followed by the quincunx filter bank (Fig. 2). To decrease artifacts due to the Gibbs-like phenomenon in the DFB stage, we move downsampling and resampling to the end of the synthesis part and to the beginning of the analysis part, using the Nobel identities [3].

At each level (j) in the wavelet transform, we obtain the traditional three highpass bands corresponding to the LH, HL, and HH bands. We apply DFB with the same number of directions to each band in a given level (j). Starting from the desired maximum number of directions $N_D = 2^L$ on the finest level of the wavelet transform J, we decrease the number of directions at every other dyadic scale when we proceed through the coarser levels ($j < J$). This way, we could achieve the anisotropy scaling law; that is, $width \approx length^2$. Fig. 3 illustrates a schematic plot of the WBCT using 3 wavelet levels and L=3 directional levels. Since we have mostly vertical directions in the HL image and horizontal directions in the LH image, it might seem logical to use partially decomposed DFB with vertical and horizontal directions on the HL and LH bands, respectively. However, since the wavelet filters are not perfect in splitting the frequency space to the lowpass and highpass components, that is, not all of the directions in the HL image are vertical and in the LH image are horizontal, we use fully decomposed DFB on each band.

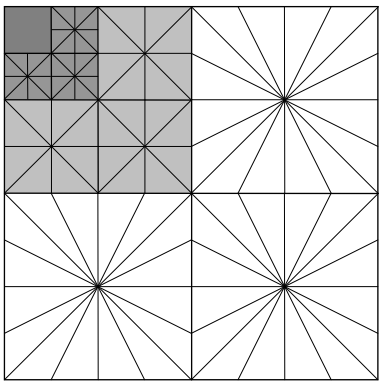

Fig. 3. A schematic plot of the WBCT using 3 dyadic wavelet levels and 8 directions at the finest level (N_D =8). The directional decomposition is overlaid the wavelet subbands.

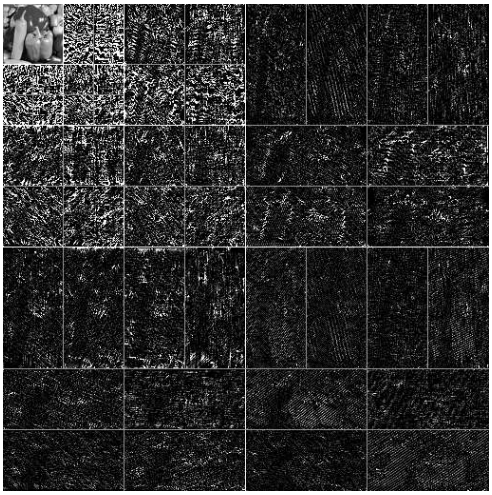

Fig. 4. The WBCT coefficients of the *Peppers* image. For better visualizing, the transform coefficients are clipped between 0 and 7.

Fig. 4 shows an example of the WBCT coefficients of the *Peppers* image. Here we used 3 wavelet levels and 8 directions at the finest level. You can see that most of the coefficients in the HL subbands are in the vertical directional subbands (the upper half of the subbands) while those in the LH subbands are in the horizontal directional subbands (the lower half of the subbands).

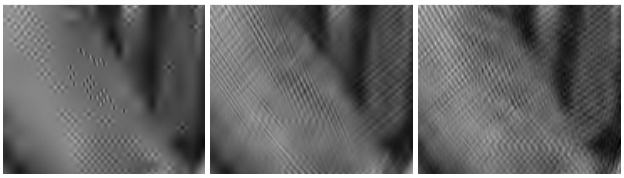

PSNR = 24.637 PSNR = 24.792 PSNR = 24.997

Fig. 5. Non-linear approximation results using 4096 coefficients for the *Barbara* image. *Left:* wavelet transform. *Middle:* contourlet transform. *Right:* wavelet-based contourlet transform. Small parts of the images are shown.

III. WBCT CODING USING SPIHT

A. Non-linear Approximation

Building an efficient transform coder requires that the corresponding transform should, at minimum, provide good non-linear approximations of the input signal [10]. Now, we demonstrate that the WBCT coefficients do provide efficient non-linear approximations of natural images, especially those containing a significant amount of textures and oscillatory patterns. We performed some non-linear approximation experiments to evaluate the WBCT in comparison with wavelets and contourlets. All of the schemes use biorthogonal Daubechies 9-7 as the subband decomposition. The contourlet transform uses 6 Laplacian pyramid subbands and 32 directions at the finest scale. The WBCT uses 5 wavelet levels and 16 directions at the finest scale. We used non-separable fan filters of support sizes 23*23 and 45*45 designed in [12]. The FIR half-band filter used for constructing fan filters is designed using the *"remez"* function in MATLAB. Our PSNR results indicate that the WBCT performs better than the contourlet transform for non-linear approximations. Further, and more importantly, the visual results show a clear improvement over wavelets and contourlets in textured regions. Fig. 5 depicts close-up images with corresponding PSNR values for the *Barbara* image. However, we observed that in some image regions the contourlet non-linear approximation results might have less distortion than the WBCT results. The frequency scrambling due to the downsampling of the highpass channel in wavelets may be one of the reasons for this observation [3][11].

B. Tree Construction Using the Repositioning Algorithm

It should be noted that the feature mentioned in Section 3.A, that is, capability of a transform to efficiently approximating an image, does not automatically result in an efficient coder [2]. The other important issue that should be taken into account is how one codes the positions of the significant coefficients (used in the non-linear approximation) efficiently. In [15], Shapiro pioneered the notion of zero-trees for coding the positions of significant wavelet coefficients. Following his work, Said and Pearlman [14] developed the SPIHT algorithm for wavelet coding of images and could achieve significant improvement over the EZW coder [8]. In the tree-based wavelet coding algorithms such as EZW and SPIHT, considering a threshold T, if a wavelet coefficient $a_{i,j}$ is *insignificant*, i.e. $|a_{i,j}| < T$, due to a self-similarity amongst the wavelet coefficients in different subbands, it is likely that its descendents at the finer wavelet scales are insignificant. A similar observation can be made about the proposed WBCT coefficients; however, the definition of the "*descendants*" of a WBCT coefficient needs to be modified (as we elaborate further below). Therefore, using this presumption, and similar to the original SPIHT algorithm, we can assign a non-significant WBCT coefficient to the *list of insignificant set* (LIS) and perform the same set partitioning algorithm as done within the SPIHT algorithm for wavelet coding. Hence, following the same approach of SPIHT, we create three sets of LIP (list of insignificant pixels), LIS, and LSP (list of significant pixels) and perform set partitioning and refining the significant pixels of the WBCT coefficients during coding.

Similar to the spatial orientation tree (*or* zero-tree) concept of wavelet coefficients in which we have a parent-child relationship along wavelet scales, one can find parent-child dependencies in other subband systems. In the case of the contourlet transform, one can assume two different parent-child relationships depending on the number of directional decompositions in the contourlet subbands [13]. If the two successive scales in which the parent and children lie have the same number of directional decompositions, then the parent and children would lie in the corresponding directional subbands; however if the scale in which the children lie has twice as many directional subbands as the scale in which the parent lies, the four children will be in two adjacent directional subbands. These two directional subbands correspond to the directional decomposition of the directional subband in which the parent is located. Due to the similarities of the WBCT to the contourlet transform, for each LH, HL, and HH subband we can assume the same parent-child relationships as illustrated in Fig. 6.

Therefore, due to differences in parent-children dependencies between the WBCT and the wavelet transform, before applying the SPIHT algorithm, we reposition the transform coefficients in the WBCT in such a way to be able to use a similar SPIHT algorithm. Fig. 7 shows an example of repositioning a radial subband in the WBCT having 8 directional decompositions. This example assumes that the coarser subband has 4 directional decompositions. In the left image of Fig. 7, we have 8 directional subbands (separated by dashed lines). Each two adjacent horizontal subbands (upper half subbands) and each two adjacent vertical subbands (lower half subbands) are corresponding to a horizontal subband and a vertical subband in the coarser scale, respectively. Therefore, for example, the children of pixel (1,1) in the first horizontal coarser subband (that is located in the upper left) are lying in the white and gray columns numbered 1 at positions (in this figure) (1,1), (1,2),(1,6), and (2,6). So, if we reposition the columns of the horizontal directional subbands and the rows of the vertical directional subbands in a manner to set the children beside each other, we can benefit from using a similar tree-based wavelet coding algorithm for the WBCT coefficients. The above example shows a simple case when we interlace the columns of horizontal subbands and rows of the vertical subbands to achieve our purpose. However, as we

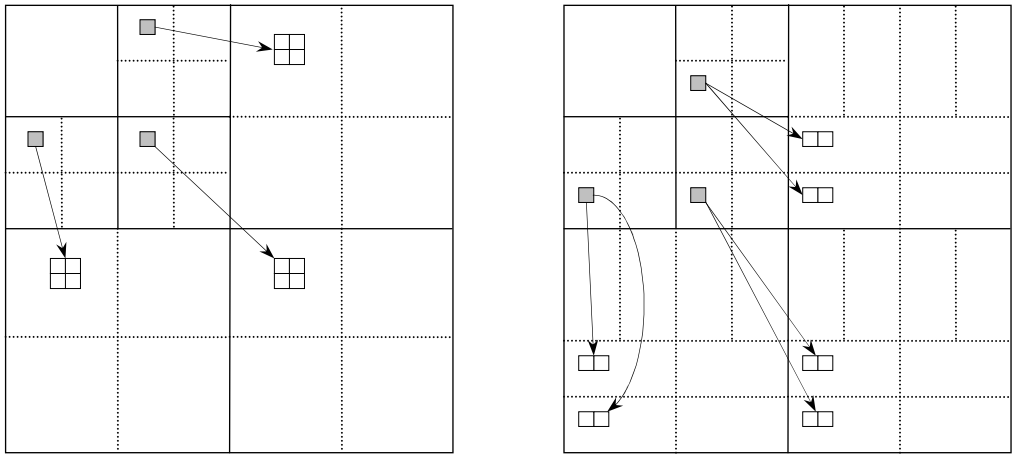

(a) (b)

Fig. 6. Two possible parent-child relationships in the WBCT. Wavelet subbands (or radial subbands in the WBCT) are separated by the solid lines and directional subbands separated by the dotted lines. (a) When the number of directional subbands are the same at the two wavelet scales. Here we have 4 directions at each wavelet subband. (b) When the number of directional subbands in the finer wavelet scale (here is 8) is twice as many as those in the coarser wavelet scale (here is 4).

move forward along the scales, the repositioning algorithm becomes more complex and we have to interlace sets of 2, 4, or any higher number of columns (rows) of the horizontal (vertical) subbands in order to maintain the descendent of a WBCT coefficient adjacent to each other similar to the wavelet coefficients.

IV. Numerical Results

We tested the proposed coding scheme as well as the original SPIHT coder on several images, each having a size of 512x512. We used the same WBCT and wavelet transform as those we used in Section 3.B for non-linear approximation experiments. An arithmetic encoder is used to entropy-code the resulting bit streams of the SPIHT algorithm. Fig. 8 shows the rate-distortion curves obtained for coding the images using the SPIHT wavelet and WBCT coders. We can see that the PSNR values for both schemes are very close. Although the wavelet coder shows a very slightly better performance in terms of PSNR values, our experiments indicated that the proposed scheme is superior in preserving textures and details in the coded images. This observation is not effectively captured by the PSNR metric. Fig. 9 shows the coded results of the *Fingerprint* image at rate $R = 0.1$ bpp. As seen, more ridges in the coded image by the proposed coder are retained. As another example, we depicted part of the *Barbara* image coded at a rate equal to 0.25 bpp in Fig. 10. This figure clearly shows the capability of the proposed coder for images consisting of mainly textures and oscillatory patterns.

V. Conclusion

We proposed the wavelet-based contourlet transform, which is a new non-redundant transform, and designed a new image coder based on the proposed WBCT transform using an SPIHT-like algorithm. Our simulation results indicated that the

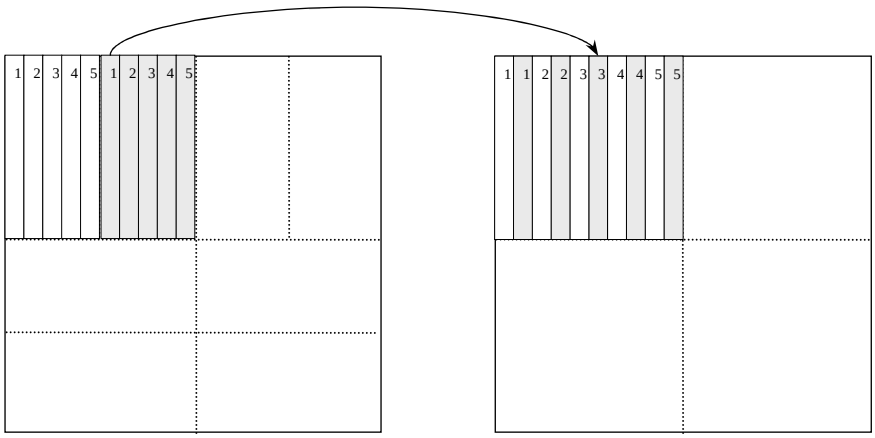

Fig. 7. An example of repositioning a radial subband in the WBCT having 8 directional subbands assuming its coarser subband is at first level and has 4 directional decompositions. In this process we combine each two adjacent directional subbands by interlacing the columns of horizontal directional subbands (upper half subbands) and the rows of vertical directional subbands (lower half subbands).

proposed coder is visually superior to the wavelet SPIHT scheme in preserving details and textures in the coded images.

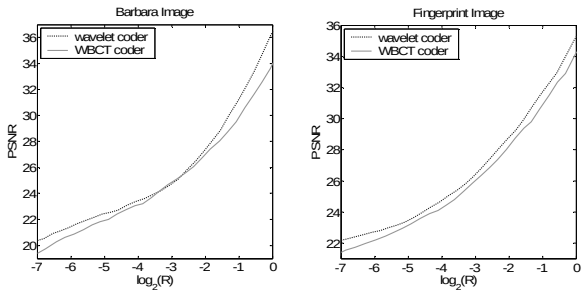

Fig. 8. Rate-distortion curves obtained for the images *Barbara* and *Fingerprint* using the SPHIT wavelet and WBCT coders.

Fig. 9. The coding results of the *Fingerprint* image at a rate equal to 0.1 bpp. *Left:* coded image using the SPIHT wavelet coder (PSNR=25.76). *Right:* coded image using the SPIHT WBCT coder (PSNR=25.38).

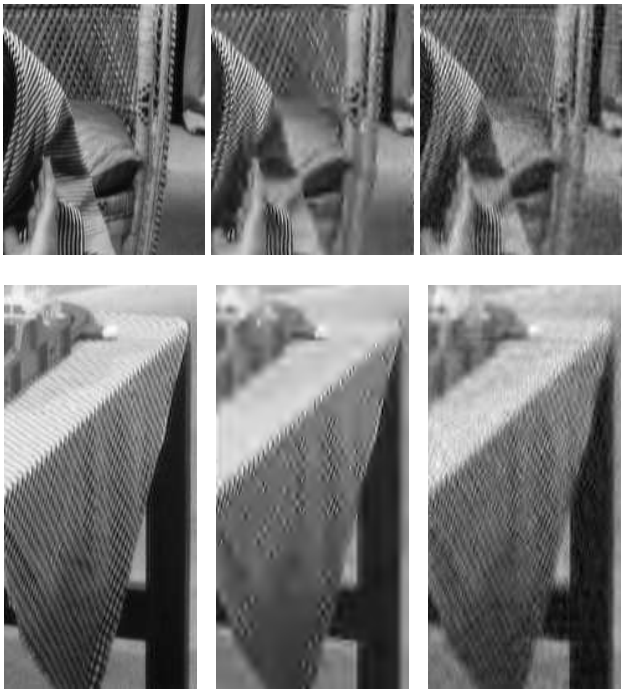

Fig. 10. Parts of the *Barbara* image coded at rate 0.25 bpp. *Left:* original image. *Middle:* result of the SPIHT coder (PSNR=27.38). *Right:* result of the proposed coder (PSNR=27).

REFERENCES

[1] E. J. Candes and D. L. Donoho, "Curvelets – a suprizingly effective nonadaptive representation for objects with edges," *in Curve and Surface Fitting*, a. Cohen, C. Rabut, and L. L. Schumaker Eds., Saint-Malo, 1999, Vanderbuilt Univ. Press.

[2] A. Cohen, I. Daubechies, O. Guleryuz, and M. Orchard, "On the Importance of Combining Wavelet-Based Non-linear Approximation with Coding Strategies," *in IEEE trans. Information Theory*, vol. 48, no. 7, pp. 1895-1921, Jul. 2002.

[3] M. N. Do, *Directional multiresolution image representations.* Ph.D. thesis, EPFL, Lausanne, Switzerland, Dec. 2001.

[4] M. N. Do and M. Vetterli, "Contourlets," in *Beyond Wavelets*, J. Stoeckler and G. V. Welland, Eds. Academic Press, New York, 2003.

[5] R. Eslami and H. Radha, "On low bit-rate coding using the contourlet transform," to be published in *Asilomar Conference on Signals, Systems, and Computers*, Pacific Grove, USA, Nov. 2003.

[6] R. Eslami and H. Radha, "The contourlet transform for image de-noising using cycle spinning," to be published in *Asilomar Conference on Signals, Systems, and Computers*, Pacific Grove, USA, Nov. 2003.

[7] P. Hong and M. J. T. Smith, "An octave-band family of non-redundant directional filter banks," *in IEEE proc. ICASSP*, vol. 2, pp. 1165-1168, 2002.

[8] Image Communication Lab., UCLA, *Wavelet Image Coding: PSNR Results.* [online] Available at http://www.icsl.ucla.edu/~ipl/psnr_results.html.

[9] Y. Lu and M. N. Do, "CRISP-contourlets: a critically sampled directional multiresolution image representation," *in proc. of SPIE conference on Wavelet Applications in Signal and Image Processing X*, San Diego, USA, August 2003.

[10] S. Mallat and F. Falzon, "Analysis of low bit-rate image transform coding," *IEEE trans. on Signal Processing*, vol. 46, no. 4, pp. 1027-1042, Apr. 1998.

[11] S. Park, M. J. T. Smith, and R. M. Mersereau, "A new directional filter bank for image analysis and classification," *in IEEE proc. ICASSP*, vol. 3, pp. 1417-1420, Mar. 1999.

[12] S. M. Phoong, C. W. Kim, P. P. Vaidyanathan, and R. Ansari, "A new class of two-channel biorthogonal filter banks and wavelet bases," *in IEEE trans. on Signal Processing*, vol. 43, no. 3, pp. 649-665, Mar. 1995.

[13] D. D.-Y. Po and M. N. Do, "Directional multiscale modeling of images using the contourlet transform," submitted to *IEEE trans. on Image Processing*, 2003.

[14] A. Said and W. A. Pearlman, "A New Fast and Efficient Image Codec Based on Set Partitioning in Hierarchical Trees," *IEEE trans. on Circuits and Systems for Video Technology*, vol. 6, pp. 243-250, June 1996.

[15] J.M. Shapiro, "Embedded image coding using zerotrees of wavelet coefficients," *IEEE trans. on Signal Processing (Special Issue, Wavelets and Signal Processing*), vol. 41, pp. 3445-3462, Dec. 1993.